

Magnetic phase diagram for the mixed-valence Eu oxide $\text{EuTi}_{1-x}\text{Al}_x\text{O}_3$ ($0 \leq x \leq 1$)Daisuke Akahoshi,^{1,2,*} Shuto Koshikawa,¹ Takuro Nagase,¹ Eiji Wada,² Kosuke Nishina,³ Ryo Kajihara,³ Hideki Kuwahara,³ and Toshiaki Saito^{1,2}¹*Department of Physics, Faculty of Science, Toho University, Funabashi, Chiba 274-8510, Japan*²*Research Center for Materials with Integrated Properties, Toho University, Funabashi, Chiba 274-8510, Japan*³*Department of Physics, Sophia University, Tokyo 102-8554, Japan*

(Received 2 June 2017; revised manuscript received 3 October 2017; published 15 November 2017)

We have investigated the magnetic properties of $\text{EuTi}_{1-x}\text{Al}_x\text{O}_3$ with $0 \leq x \leq 1$ and established a detailed magnetic phase diagram. Substitution of Ti^{4+} with Al^{3+} , which oxidizes magnetic Eu^{2+} ($J = 7/2$) into nonmagnetic Eu^{3+} ($J = 0$), turns the antiferromagnetic insulating ground state ($x = 0$) into the ferromagnetic (FM) insulating one ($0.10 \leq x \leq 0.50$). The $\text{Eu}^{2+}/\text{Eu}^{3+}$ mixed valence is indispensable for the FM behavior. In $0.10 \leq x \leq 0.33$, the Curie temperature T_C has a plateau at ~ 4 K, and the FM correlation is most enhanced around $x = 0.25$. In $0.33 \leq x \leq 1$, Al^{3+} substitution suppresses the FM correlation due to the dilution of magnetic Eu^{2+} ions. Our present results would provide useful information for magnetoelectric phase control of EuTiO_3 -based compounds.

DOI: [10.1103/PhysRevB.96.184419](https://doi.org/10.1103/PhysRevB.96.184419)**I. INTRODUCTION**

Materials that exhibit strong coupling between electric and magnetic properties have attracted much interest for their fundamental physics as well as potential application for spintronic devices [1]. Perovskite Eu titanate EuTiO_3 (ETO) is one of such materials [2]. ETO has a cubic perovskite structure with a space group of $Pm\bar{3}m$ around room temperature, undergoing the antiferrodistortive (AFD) transition [the transition from the cubic ($Pm\bar{3}m$) to tetragonal ($I4/mcm$) perovskite structures] below room temperature [3–5]. Due to the absence of $3d$ electrons, ETO is an insulating oxide, and exhibits a quantum paraelectric (PE) behavior at low temperatures [6]. The structural and electric properties of ETO are analogous to those of SrTiO_3 [7–9]. The magnetism of ETO arises from strongly localized $4f$ electrons of Eu^{2+} ($J = S = 7/2$), since Ti^{4+} has no $3d$ electron. In spite of the positive Curie-Weiss temperature $\theta_{\text{CW}} \simeq +3$ K, ETO undergoes the antiferromagnetic (AFM) transition at the Néel temperature $T_N \simeq 5$ K, indicating that an underlying ferromagnetic (FM) interaction exists [10,11]. In the vicinity of T_N , ETO exhibits a large magnetocapacitance effect: application of magnetic fields increases the dielectric constant by $\sim 7\%$ [6]. The AFD instability is considered to play a significant role in the magnetoelectric (ME) behavior in ETO [12].

Fennie and Rabe theoretically predicted that by applying an epitaxial strain the ground state of ETO changes from the AFM-PE insulator to a ferromagnetic-ferroelectric (FM-FE) one [13]. Lee *et al.* experimentally showed that tensilely strained ETO film grown on DyScO_3 substrate is a multiferroic material that has FM and FE orders simultaneously [2]. Furthermore, Ryan *et al.* demonstrated that the magnetic ground state of compressively strained ETO film grown on $(\text{LaAlO}_3)_{0.29}-(\text{SrAl}_{0.5}\text{Ta}_{0.5}\text{O}_3)_{0.71}$ substrate can be controlled by electric fields [14].

Chemical substitution as well as an epitaxial strain is an effective method for controlling physical properties of

materials. In our previous work, we have synthesized $\text{EuTi}_{1-x}\text{Al}_x\text{O}_3$ (ETAO) with $0 \leq x \leq 0.10$ and $\text{EuTi}_{1-x}\text{Ga}_x\text{O}_3$ (ETGO) with $0 \leq x \leq 0.10$ and investigated the magnetic properties [15]. Both ETAO and ETGO have the mixed valence of $\text{Eu}^{2+}/\text{Eu}^{3+}$ as a result of substitution of Ti^{4+} with heterovalent Al^{3+} and Ga^{3+} , and they exhibit FM insulating behavior below ~ 4 K while ETO substituted with isovalent Zr^{4+} does not. This result indicates that the $\text{Eu}^{2+}/\text{Eu}^{3+}$ mixed valence significantly contributes to the FM behavior. In this paper, we have prepared ETAO with $0 \leq x \leq 1$ using a solid-state reaction and arc-melting methods, and elaborately investigated the magnetic properties. As a result, the overall phase diagram for the ETAO system has been established.

II. EXPERIMENT

Polycrystalline samples of ETAO with $0 \leq x \leq 0.10$ were synthesized by a solid-state reaction [15]. ETAO with $0.10 < x \leq 1$ were prepared in polycrystalline form by the following procedure. Eu_2O_3 , TiO_2 , and Al_2O_3 were used as starting materials. Mixed powders of appropriate molar ratio are pressed into pellets, and then sintered at 1673 K under 5% H_2 -Ar flow. At this stage, ETAO with $0.10 < x \leq 1$ contains a significant amount of impurity phases. These sintered pellets were melted by an arc furnace under Ar atmosphere. These arc-melted samples were annealed under 5% H_2 -Ar flow at 1723 K. The powder x-ray-diffraction (XRD) profiles indicate that all ETAO samples prepared in this study have single phase perovskite structures. Magnetic properties were measured by a Quantum Design magnetic property measurement system. ETAO shows insulating transport behavior in the whole region of x . We note that ETGO with $x > 0.10$ could not be obtained by this procedure.

III. RESULTS

We exhibit the XRD patterns for ETAO with $x = 0$ – 0.25 and 0.33 – 1 collected at room temperature in Figs. 1(a) and 1(b), respectively. The simulated XRD patterns for the end members, ETAO with $x = 0$ (ETO) and 1 (EuAlO_3), are

*daisuke.akahoshi@sci.toho-u.ac.jp

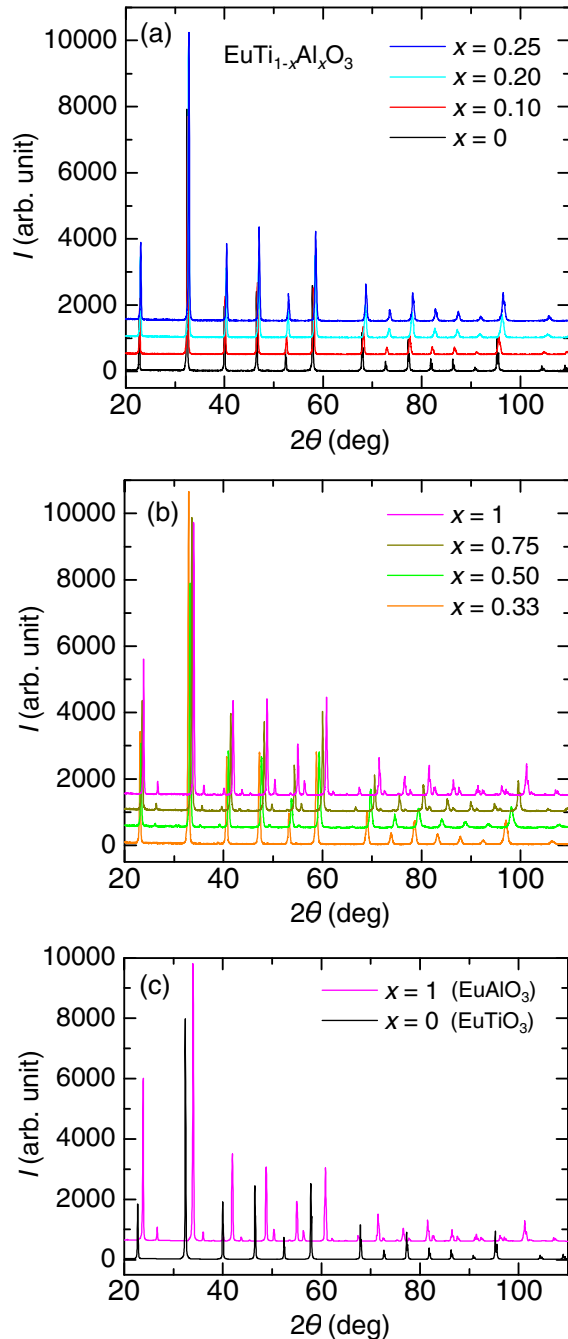


FIG. 1. Powder x-ray-diffraction profiles for $\text{EuTi}_{1-x}\text{Al}_x\text{O}_3$ with (a) $0 \leq x \leq 0.25$ and (b) $0.33 \leq x \leq 1$ at room temperature. (c) Simulated powder XRD profiles for the end members, EuTiO_3 (ETAO with $x = 0$) and EuAlO_3 (ETAO with $x = 1$).

also shown in Fig. 1(c) for comparison. As clearly seen from the XRD patterns, the positions of Bragg peaks monotonically shift to higher angles with increasing x , since substitution of Ti^{4+} with smaller Al^{3+} and concomitant oxidization of Eu^{2+} into Eu^{3+} reduce the unit-cell volume of ETAO. The XRD profiles for ETO and EuAlO_3 can be indexed as a simple cubic perovskite structure with a space group $Pm\bar{3}m$ [4,5,10] and as an orthorhombic perovskite structure with a space group $Pbnm$ [16], respectively. ETAO retains the cubic perovskite structure in $0 \leq x \leq 0.25$ [Fig. 1(a)]. In $x = 0.33$, the Bragg

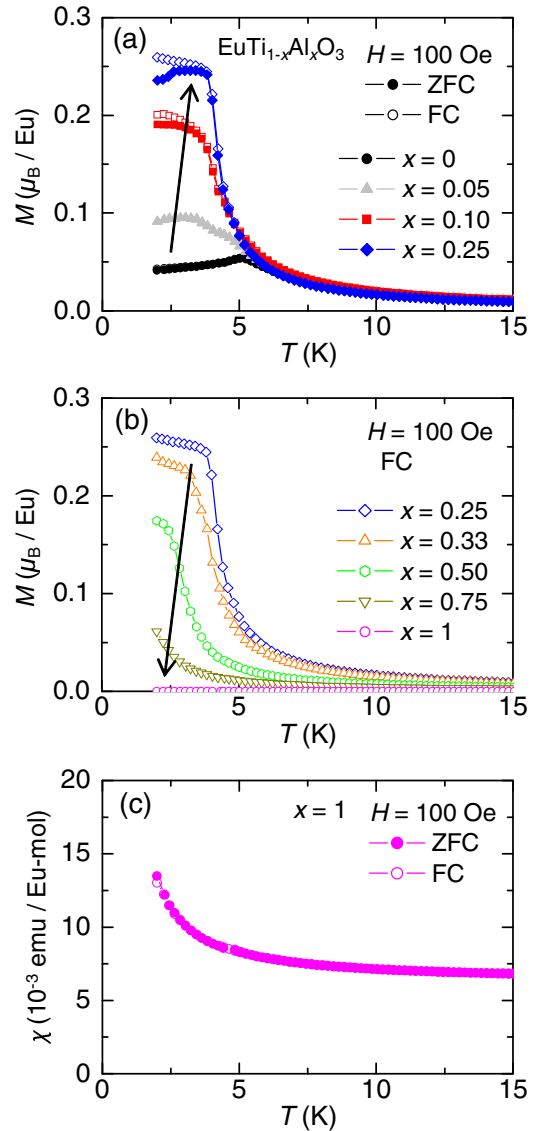


FIG. 2. Temperature (T) dependence of magnetization (M) of (a) ETAO with $0 \leq x \leq 0.25$ and (b) $0.25 \leq x \leq 1$ measured at $H = 100$ Oe. ZFC and FC denote zero-field cooling and field cooling, respectively. (c) T dependence of magnetic susceptibility (χ) of ETAO with $x = 1$ (i.e., EuAlO_3) measured at $H = 100$ Oe.

peaks due to the orthorhombic distortion start to appear [Fig. 1(b)], indicating that the structural transition from the cubic to the orthorhombic perovskite occurs around $x = 0.33$. In the intermediate region of $0.33 \leq x \leq 0.50$, the Bragg peaks are rather broadened, which is probably attributed to lattice disorder arising from a large mismatch in the ionic radii between Ti^{4+} and Al^{3+} . Rietveld analysis using the RIETAN-FP program [17] indicates that the cubic and orthorhombic phases coexist in $x = 0.33$ and that ETAO with $x = 0.5$ has the single phase perovskite structure with orthorhombic distortion.

Figure 2 shows the temperature dependence of the magnetization (M) of ETAO. Here ZFC and FC denote zero-field cooling and field cooling, respectively. The M of ETAO with $x = 0$ (ETO) shows a cusp due to the AFM transition at $T_N = 5.2$ K. Al^{3+} substitution creates a FM component below T_N as previously reported [15]. In $x = 0.05$, the M below

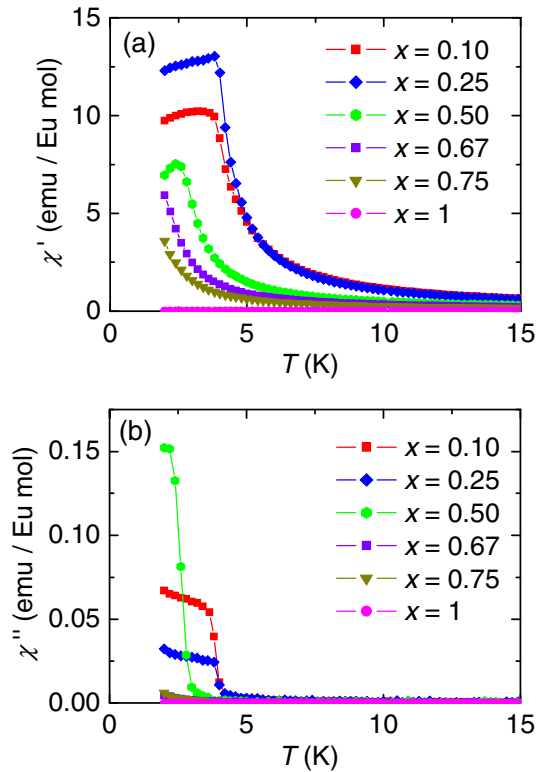


FIG. 3. (a) Real component χ' and (b) imaginary component χ'' of ac χ for ETAO with $0.10 \leq x \leq 1$ measured at frequency $f = 1$ Hz and field amplitude $h = 3$ Oe.

~ 4 K is increased compared with that of ETO, but the AFM cusp is still observed around 5 K. This result suggests that in the low-doped region $0 < x < 0.10$ the AFM and FM phases coexist or the AFM and FM transitions successively occur. In $x = 0.10$, the M below ~ 4 K is further increased, and the AFM cusp is no longer observed, indicating that the FM phase is dominant. In $0 \leq x \leq 0.25$, in spite of the decrease in magnetic Eu^{2+} ions, the M at low temperatures is increasing with increasing x , reaching the maximum around $x = 0.25$ [Fig. 2(a)]. In $0.25 < x \leq 1$, an increase in x monotonically suppresses the M at low temperatures [Fig. 2(b)]. In ETAO with $x = 1$ (EuAlO_3), all magnetic Eu^{2+} ions are oxidized into nonmagnetic Eu^{3+} ions, so that the M is much smaller than that of ETAO compounds containing Eu^{2+} ions.

The temperature dependence of the magnetic susceptibility χ of EuAlO_3 is shown in Fig. 2(c). EuAlO_3 exhibits paramagnetic behavior, which arises from the Van Vleck paramagnetism of Eu^{3+} , as previously reported [16]. No magnetic anomaly indicative of a magnetic transition is observed in the measured temperature range. The magnitude of the χ is $\sim 7 \times 10^{-3}$ emu/ Eu^{3+} mol, which is comparable with those of other Eu^{3+} -based compounds such as EuBO_3 , Eu_2O_3 , and EuF_3 [18]. The slight upturn in the χ at low temperatures is probably attributed to Eu^{2+} impurity arising from a slight amount of oxygen deficiency and/or second phase.

Figure 3 presents the ac χ of ETAO. The temperature dependence of the real component χ' of the ac χ [Fig. 3(a)] shows a similar trend to that of the M (Fig. 2). Around $x = 0.25$, the χ' at low temperatures is most enhanced like

the case of the M . The imaginary components χ'' of the ac χ of ETAO with $x = 0.10$ and 0.25 show an abrupt change around 4 K, indicating that the magnetic transition (i.e., the FM transition) occurs at the temperature [Fig. 3(b)]. Here the Curie temperature T_C is determined from the derivative of the χ'' ($d\chi''/dT$). The T_C 's of ETAO with $x = 0.10$ – 0.33 almost coincide with each other ($T_C = 4.2$ – 4.3 K). In $x = 0.50$, the T_C is lowered by ~ 1 K, and the χ'' below the T_C is much larger than that in $x = 0.25$, which might be attributed to the emergence of a magnetic glassy component resulting from the dilution of magnetic Eu^{2+} ions. In $0.67 \leq x \leq 1$, the abrupt change in the χ'' is no longer observed in the measured temperature range, suggesting that the T_C is below 2 K and that the FM phase disappears between $x = 0.67$ and 1. However, even in $x = 0.75$, the χ'' exhibits a slight upturn below ~ 3 K, which probably originates from Eu^{2+} impurity or might be attributed to the precursor of the FM transition.

Figure 4(a) exhibits the magnetization curves of ETAO with $0 \leq x \leq 0.75$ measured at 2 K. All the magnetization curves show saturation behavior without an appreciable hysteresis loop. The saturation M is monotonically decreasing toward zero with increasing x . The M at $H = 50$ kOe (M_{sat}) is plotted as a function of x in Fig. 4(b). The M_{sat} shows a linear decrease, almost coinciding with the expected value of $M_{\text{sat}} = 7\mu_B(1-x)$. This result evidences that ETAO has the mixed valence of $\text{Eu}^{2+}/\text{Eu}^{3+}$ in $0 < x < 1$. In order to compare the saturation rates of the M , we show the magnetic field dependence of the M divided by the M_{sat} in Fig. 4(c). In $0 \leq x \leq 0.25$, Al^{3+} substitution lowers the magnetic field required to saturate the M , and the M is most easily saturated around $x = 0.25$. With increasing x from 0.25, the saturation magnetic field is increasing. From this result, one can conclude that the FM correlation is most enhanced around $x = 0.25$. This conclusion is consistent with the results shown in Figs. 2 and 3.

We present the magnetic phase diagram for ETAO established from the present results in Fig. 5. The θ_{CW} , obtained from the Curie-Weiss fitting, is also plotted except for that of EuAlO_3 (ETAO with $x = 1$) in Fig. 5. The ground state of the pristine compound ETO (ETAO with $x = 0$) is an AFM insulator. By partial substitution of Ti^{4+} with Al^{3+} , the FM component emerges below T_N . In the low-doped region $0 < x < 0.1$, the AFM and FM phases coexist or the successive magnetic transitions occur. In $x \geq 0.10$, the FM phase is dominant. The x dependence of the T_C has a plateau around 4 K in $0.10 \leq x \leq 0.33$. In $x > 0.33$, the effect of the dilution of magnetic Eu^{2+} ions is prominent. In this region, the T_C is decreasing toward zero with increasing x . As seen from the result that the θ_{CW} is positive in the whole region of x (except for $x = 1$), the FM interaction is dominant in the ETAO system. The θ_{CW} of ETO is $+3.17$ K, which is the same as the value previously reported [6]. In $0 \leq x \leq 0.25$, the θ_{CW} is rising with increasing x , reaching the maximum value of $\theta_{\text{CW}} = +3.80$ K around $x = 0.20$ – 0.25 . This result also indicates that the FM correlation is most enhanced around $x = 0.25$. A further increase in x from 0.25 reduces the θ_{CW} , and the extrapolated θ_{CW} at $x = 1$ is about $+1$ K. In $0.10 \leq x \leq 0.50$, the θ_{CW} is slightly lower than the T_C , although, in general, it is slightly higher than the T_C . In the present case, strong competition between the AFM and FM interactions probably suppresses the θ_{CW} .

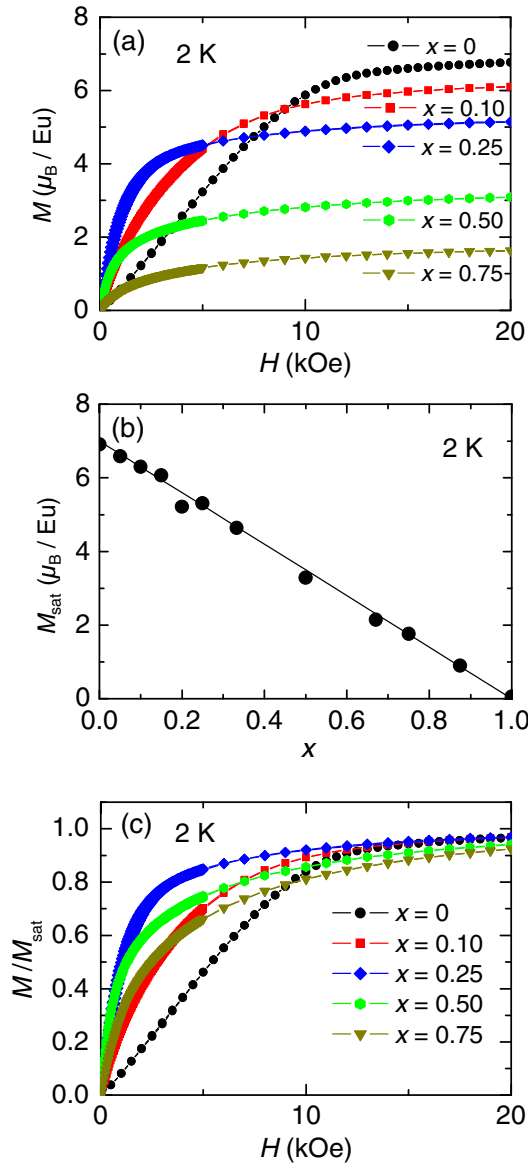


FIG. 4. (a) Magnetic field (H) dependence of M for ETAO with $0 \leq x \leq 0.75$ at 2 K. (b) x dependence of M_{sat} for ETAO with $0 \leq x \leq 1$. M_{sat} represents M at $H = 50$ kOe. (c) H dependence of M/M_{sat} for ETAO with $0 \leq x \leq 0.75$ at 2 K.

IV. DISCUSSION

First, we discuss the origin of the FM behavior of ETAO. In the parent compound ETO, the AFM and underlying FM interactions compete with each other [10,11]. Therefore, the magnetic property of ETO is sensitive to perturbations caused by chemical substitution or epitaxial strain. For example, electron-doped ETO such as $\text{Eu}_{0.9}\text{La}_{0.1}\text{TiO}_3$ [19], $\text{EuTi}_{1-x}\text{Nb}_x\text{O}_3$ with $x \geq 0.2$ [20–22], and $\text{EuTiO}_{3-x}\text{H}_x$ with $0.07 \leq x \leq 0.3$ [23] exhibit FM metallic behavior. In these cases, the origin of the FM interaction arises from Ruderman-Kittel-Kasuya-Yoshida (RKKY) interaction between localized Eu $4f$ spins and itinerant Ti $3d$ or Nb $4d$ electrons. On the other hand, in the case of ETAO, the resistivity is highly insulating because of the absence of d electrons. Therefore, it is clear that RKKY interaction is irrelevant to the emergence of the FM

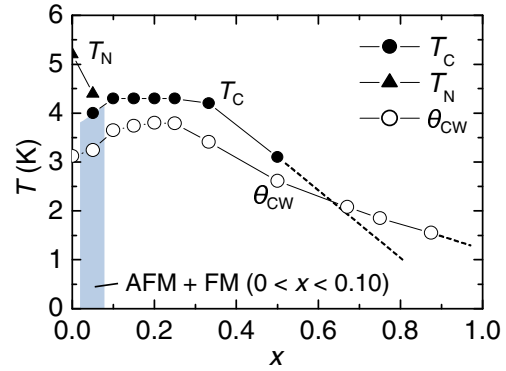


FIG. 5. The magnetic phase diagram for ETAO. Closed circles, triangles, and open circles represent Curie temperature T_C , Néel temperature T_N , and Curie-Weiss temperature θ_{CW} , respectively.

phase of ETAO. On the other hand, substitution of Eu^{2+} with nonmagnetic alkaline-earth ions such as Ca^{2+} , Sr^{2+} , and Ba^{2+} , which corresponds to the dilution of magnetic Eu^{2+} ions, does not induce an AFM to FM transition [24–26] while ETAO, in which Eu^{2+} is diluted with nonmagnetic Eu^{3+} , exhibits the FM insulating state as demonstrated above. This means that the origin of the FM behavior cannot be explained by the effect of the magnetic dilution.

In our previous paper, we proposed that the mixed valence of $\text{Eu}^{2+}/\text{Eu}^{3+}$ is indispensable for the FM behavior and that a FM super-super-exchange process between Eu^{2+} ions through Eu^{3+} stabilizes the FM interaction [15]. Another possible explanation for the origin of the FM behavior is that structural distortion resulting from Al^{3+} substitution stabilizes the FM phase. In the case of ETO film on DyScO_3 , large structural distortion ($\sim 1\%$ tensile strain) enhances the FM interaction and simultaneously generates the polarization through Eu-Ti-Eu bond alignment [14]. We confirmed that the crystal structure of ETAO with $x = 0.25$, which has the FM ground state with $T_C = 4.3$ K, remains cubic at 87 K by powder XRD measurements. In addition, no anomaly indicative of a phase transition is observed between $T_C = 4.3$ and 87 K in the magnetization and heat capacity measurements. These results show that Al^{3+} substitution suppresses the AFD (tetragonal) transition characteristic of ETO and that ETAO with $x = 0.25$ retains the cubic perovskite structure immediately above T_C . If ETAO with $x = 0.25$ undergoes the structural transition at T_C , large structural distortion cannot be expected since the FM transition is of second-order type. From these results, we conclude that the origin of the FM behavior of ETAO is different from that of ETO film on DyScO_3 and that the $\text{Eu}^{2+}/\text{Eu}^{3+}$ mixed valence is essential for the ferromagnetism of ETAO. Furthermore, in our preliminary study, a FE transition is not observed in ETAO with $x = 0.25$ as mentioned below, which also supports the above conclusion.

In the heavily doped region $0.5 \leq x \leq 1$, Al^{3+} substitution weakens the FM correlation as demonstrated above, which can be naturally explained by the magnetic dilution. However, at the same time, the orthorhombic distortion is stabilized in this region, so that we cannot exclude a possibility that not only the magnetic dilution but also the orthorhombic distortion

contributes to the suppression of the FM correlation in heavily doped ETAO.

Besides the origin of the FM behavior, there are some other issues to be addressed.

(1) Does charge ordering of $\text{Eu}^{2+}/\text{Eu}^{3+}$ occur in ETAO with the commensurate x such as $x = 1/3, 1/4$, and $1/2$? If so, it would be interesting to investigate the ME properties of charge ordered ETAO. However, no sign of a charge order transition is observed in our present data in the measured temperature range of 2–400 K.

(2) How does the $\text{Eu}^{2+}/\text{Eu}^{3+}$ mixed valence affect the ME properties of ETAO? In order to solve these issues, a detailed study using ETAO in single-crystalline form is required, which would lead to finding some intriguing ME phenomena arising from the close interplay between the lattice, magnetism, and $\text{Eu}^{2+}/\text{Eu}^{3+}$ mixed valence.

Lastly, we briefly report our preliminary study of the electric properties of single-crystalline ETAO with $x \approx 0.25$. The dielectric constant ϵ at low temperatures, measured at frequency $f = 100$ kHz, is smaller than that of the parent compound ETO, suggesting that Al^{3+} substitution suppresses the quantum paraelectricity of ETO. The temperature dependence of the ϵ does not show any anomaly indicative of a FE transition in the temperature range from ~ 2 to ~ 100 K. Above ~ 100 K, we could not measure the electric properties of ETAO due to leakage current. This preliminary study was carried out using a single-crystalline sample with poor quality.

In order to investigate the detailed electric properties of ETAO, a single-crystalline sample with high quality is needed.

V. SUMMARY

In this paper, we have investigated the magnetic properties of $\text{EuTi}_{1-x}\text{Al}_x\text{O}_3$ with $0 \leq x \leq 1$, and established the magnetic phase diagram. The pristine EuTiO_3 (ETAO with $x = 0$) is an antiferromagnetic insulator with the Néel temperature $T_N \simeq 5$ K. Substitution of Ti^{4+} with Al^{3+} oxidizes magnetic Eu^{2+} ($J = 7/2$) into nonmagnetic Eu^{3+} ($J = 0$), and concomitantly the ferromagnetic correlation is enhanced. The $\text{Eu}^{2+}/\text{Eu}^{3+}$ mixed valence is an essential ingredient for the FM behavior. ETAO with $0.10 \leq x \leq 0.50$ exhibits FM insulating behavior, and the Curie temperature T_C has a plateau around 4 K in $0.10 \leq x \leq 0.33$. The result of the magnetization curve measurements indicates that the FM correlation is most enhanced around $x = 0.25$. With increasing x from 0.33 to 1, the T_C is decreasing toward zero due to the dilution of magnetic Eu^{2+} ions. The orthorhombic distortion resulting from Al^{3+} substitution also might contribute to the suppression of the FM correlation. The present results would provide a new route for magnetoelectric phase control of EuTiO_3 -based compound.

ACKNOWLEDGMENT

This paper was supported by Japan Society for the Promotion of Science KAKENHI Grant No. 26400370.

-
- [1] M. Fiebig, *J. Phys. D* **38**, R123 (2005).
- [2] J. H. Lee, L. Fang, E. Vlahos, X. Ke, Y. W. Jung, L. F. Kourkoutis, J.-W. Kim, P. J. Ryan, T. Heeg, M. Roeckerath, V. Goian, M. Bernhagen, R. Uecker, P. C. Hammel, K. M. Rabe, S. Kamba, J. Schubert, J. W. Freeland, D. M. Muller, C. J. Fennie, P. Schiffer, V. Gopalan, E. Johnston-Halperin, and D. G. Schlom, *Nature (London)* **466**, 954 (2010).
- [3] A. Bussmann-Holder, J. Köhler, R. K. Kremer, and J. M. Law, *Phys. Rev. B* **83**, 212102 (2011).
- [4] M. Allietta, M. Scavini, L. J. Spalek, V. Scagnoli, H. C. Walker, C. Panagopoulos, S. S. Saxena, T. Katsufuji, and C. Mazzoli, *Phys. Rev. B* **85**, 184107 (2012).
- [5] V. Goian, S. Kamba, O. Pacherová, J. Drahoš, L. Palatinus, M. Dušek, J. Rohlíček, M. Savinov, F. Laufek, W. Schranz, A. Fuiith, M. Kachlík, K. Maca, A. Shkabko, L. Sagarna, A. Weidenkaff, and A. A. Belik, *Phys. Rev. B* **86**, 054112 (2012).
- [6] T. Katsufuji and H. Takagi, *Phys. Rev. B* **64**, 054415 (2001).
- [7] K. A. Müller and H. Burkard, *Phys. Rev. B* **19**, 3593 (1979).
- [8] H. Unoki and T. Sakudo, *J. Phys. Soc. Jpn.* **23**, 546 (1967).
- [9] H. Thomas and K. A. Müller, *Phys. Rev. Lett.* **21**, 1256 (1968).
- [10] C.-L. Chien, S. DeBenedetti, and F. D. S. Barros, *Phys. Rev. B* **10**, 3913 (1974).
- [11] T. R. McGuire, M. W. Shafer, R. J. Joenk, H. A. Alperin, and S. J. Pickart, *J. Appl. Phys.* **37**, 981 (1966).
- [12] J.-W. Kim, P. Thompson, S. Brown, P. S. Normile, J. A. Schlueter, A. Shkabko, A. Weidenkaff, and P. J. Ryan, *Phys. Rev. Lett.* **110**, 027201 (2013).
- [13] C. J. Fennie and K. M. Rabe, *Phys. Rev. Lett.* **97**, 267602 (2006).
- [14] P. J. Ryan, J.-W. Kim, T. Birol, P. Thompson, J.-H. Lee, X. Ke, P. S. Normile, E. Karapetrova, P. Schiffer, S. D. Brown, C. J. Fennie, and D. G. Schlom, *Nat. Commun.* **4**, 1334 (2013).
- [15] D. Akahoshi, H. Horie, S. Sakai, and T. Saito, *Appl. Phys. Lett.* **103**, 172407 (2013).
- [16] D. Petrov, B. Angelov, and V. Lovchinov, *J. Alloys Compd.* **509**, 5038 (2011).
- [17] F. Izumi and K. Momma, *Solid State Phenom.* **130**, 15 (2007).
- [18] Y. Takikawa, S. Ebisu, and S. Nagata, *J. Phys. Chem. Solids* **71**, 1592 (2010).
- [19] T. Katsufuji and Y. Tokura, *Phys. Rev. B* **60**, R15021 (1999).
- [20] K. Ishikawa, G. Adachi, and J. Shiokawa, *Mater. Res. Bull.* **18**, 257 (1983).
- [21] L. Li, H. Zhou, J. Yan, D. Mandrus, and V. Keppens, *APL Materials* **2**, 110701 (2014).
- [22] L. Li, J. R. Morris, M. R. Koehler, Z. Dun, H. Zhou, J. Yan, D. Mandrus, and V. Keppens, *Phys. Rev. B* **92**, 024109 (2015).
- [23] T. Yamamoto, R. Yoshii, G. Bouilly, Y. Kobayashi, K. Fujita, Y. Kususe, Y. Matsushita, K. Tanaka, and H. Kageyama, *Inorg. Chem.* **54**, 1501 (2015).
- [24] N. L. Henderson, X. Ke, P. Schiffer, and R. E. Schaak, *J. Solid State Chem.* **183**, 631 (2010).
- [25] T. Guguchia, H. Keller, A. Bussmann-Holder, J. Köhler, and R. K. Kremer, *Eur. Phys. J. B* **86**, 409 (2013).
- [26] K. Rubi, P. Kumar, D. V. Maheswar Repaka, R. Chen, J.-S. Wang, and R. Mahendiran, *Appl. Phys. Lett.* **104**, 032407 (2014).